Multi-Physics Simulations for Triboelectric Charging of Display Panels During the Roller Transfer Process

Ki-Hyuk Kim (1) (2), David Pommerenke (2), Yingjie Gan (3) (2), Nam-Hee Goo (1), SeukWhan Lee (1)

(1) Samsung Display, Co., Ltd., Nongseo, Giheung, Gyeonggi 446-811, KOREA

(2) EMC Laboratory, Missouri University of Science and Technology, 4000 Enterprise Dr., Rolla, MO 65401, USA
tel.: 573-578-3916, fax: 573-341-4532, e-mail: kimkih@mst.edu, davidjp@mst.edu

(3) School of Science, Wuhan University of Technology, Wuhan, 430070, CHINA

50 Words Abstract - A multi-physics simulation methodology for triboelectric charging during the roller transfer process of display panels is proposed. Electrical and mechanical models for triboelectric charging are developed. Comparisons between the measured and the simulated results are conducted for the transient triboelectric charges of the display panels.

I. Introduction

There are several contact and separation steps during the display manufacturing process which increase productivity and automate manufacturing processes, such as the roller transfer of display panels and lift-up of display panels from vacuum stages. However, the glass for display panels is an insulating material in contrast to the dissipative silicon substrates; therefore, it is hard to bleed off the accumulated trioboelectric charges that accumulate.

Triboelectric charging is a physical phenomenon that has been known for thousands of years. Principles of triboelectric charging are applied in laser printing toners, electrophotography, energy harvesting devices, material separations, textile processing, pharmaceuticals, and granular flow processing. However, mechanisms of triboelectric charging are not completely understood [1]. Theoretical modeling and experimental work was conducted to address triboelectric charging of display panels [2, 3]. However, based on the authors' survey there are few simulation approaches for the analysis of triboelectric charging of display panels.

In this work, a multi-physics simulation methodology for triboelectric charging of display panels during the roller transfer process is proposed. The electrical and mechanical modeling of the roller transfer process is included, and simulation results for the transient triboelectric charges and the E-field distributions on the display panel are shown.

II. Simulation Framework for Triboelectric Charging of Display Panels During Roller Transfer

Triboelectric charging of display panels during the roller transfer process is a multi-physics problem, i.e., the accumulated charges on display glass are dependent not only on the electrical properties of materials such as (effective) work functions, surface states and contact capacitances, but also on the mechanical properties such as friction, contact pressure and area between the glass and the rollers. In addition, the problem is not a static, but a time-dependent event. Typical properties of triboelectric charging of display panels during the roller transfer process and related physics and simulation parameters are summarized in Table 1 based on previously published experimental works [1-4].

Although several simulation tools for multi-physics problems are commercially available such as COMSOL, there are few well-defined simulation models for triboelectric charging of display panels and the physical mechanisms are not clearly defined yet. It would be good to verify the proposed simulation methodology first and then implement it into the commercial multi-physics software by adopting the analytical modeling approaches.

Fig. 1 shows the flow chart of the proposed simulation methodology for triboelectric charging of display panels during the roller transfer process. First, the

electrical and the mechanical properties of the glass and the rollers such as (effective) work functions, empirical parameters for triboelectric charging, dimensions and velocities of the roller transfer system, Young's moduli and passion ratios, and so on are required to calculate the number of contacts, the contact area between the glass and the rollers, and the triboelectric charges at a given time. The triboelectric charges consist of contact and separation and frictional charges which are explained in this section. The variations of the roller diameters due to manufacturing tolerances and wear out are not considered in this work. The electrical and mechanical calculations are repeated until the charge calculation time is equal to the given E-field calculation time. After finishing the calculation of the charge distribution on the bottom of the display panel, the E-field distribution is calculated using a 3D electrostatic field simulator.

Table 1: Properties of Triboelectric Charging of Display Panels During Roller Transferring Process

Property	Related physics	Parameter
Q↑ as v_{tran}↑ , v_{tran}: transfer velocity	Frictional charging/ Distance [2, 3]	v_{tran}
Q↑ as t_{acc}/t_{dec}↓ , t_{acc}/t_{dec}: acceleration/ deceleration time	Frictional charging (not clearly explained) [2, 3]	t_{acc} and t_{dec}
Q (insulating, large d_{roller}) > Q (dissipative, small d_{roller}) , d_{roller}: diameter of roller	Different roller resistance [2]	d_{roller} and Types of materials
Q↑ as Area↑	Contact area [1]	Mass of glass

A. Modeling for Triboelectric Charging of Display panels

1. Modeling of Electrical Properties

Although the phenomenon of triboelectric charging has been described even in ancient times, there are few well-defined physical models for triboelectric charging between insulating materials. Triboelectric charging between metals or metal-to-insulator materials are well explained using the concept of work functions or effective work functions; however, many different charging mechanisms have been proposed such as electron transfer, ion transfer, and material transfer in order to physically explain triboelectric charging between insulating materials [1].

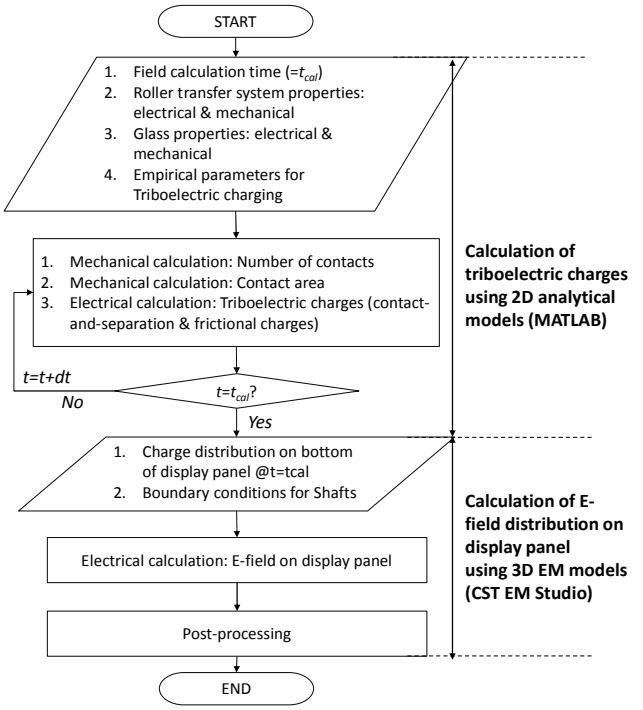

Figure 1: Proposed Simulation Methodology for Triboelectric Charging of Display Panel during Roller Transfer.

In this work, empirical modeling approaches [1, 4] are adopted to model the triboelectric charging: the empirical model consists of the charge transfer and the discharge terms, and requires experimental data to fit its coefficients. The driving force for the charge transfer is the difference in surface voltage between two materials and charges on the materials. The equation for net charge transfer is derived as [1]

$$\frac{dq}{dn} = \frac{dq_c}{dn} + \frac{dq_l}{dn}$$

$$= -\left(k_c \cdot k_i \cdot C_c + \frac{k_l}{f}\right) q + k_c \cdot C_c \cdot V_c \qquad (1)$$

where n is the number of contacts; q_c and q_l are the generated and the leakage charges of the triboelectric charging process, respectively; C_c is the contact capacitance between two materials; V_c is the (effective) work function difference; f is the frequency of the triboelectric charging process; and k_c, k_i, and k_l are proportional constants for the generated, the leakage, and the image charges, respectively. Solving (1) with the initial condition $q=q_0$ when $n=0$, gives the following equation,

$$q(n) = q_0 exp\left(-\frac{n}{n_0}\right) + q_\infty \left\{1 - exp\left(-\frac{n}{n_0}\right)\right\} \qquad (2)$$

which is used to calculate the triboelectric charges between the glass and the rollers, where n_0 is the characteristic number of the triboelectric charging, q_0 is the initial charges on the glass, and q_∞ is the saturated charges on the glass. Both the characteristic number of triboelectric charging and the saturated charges are functions of the capacitance between two materials, the contact area, the frequency of the triboelectric charging process, and the (effective) work function differences as shown in (3) and (4)

$$n_0 = \frac{1}{k_c k_i C_c + {k_l}/{f}}, q_\infty = \frac{V_c}{k_i + {k_l}/{k_c C_c f}} \quad (3)-(4).$$

It is important to note that the proportional constants k_c, k_i, and k_l are empirical parameters and the contact area between two materials should be known in order to calculate the capacitance between them.

Equations (1)–(4) were originally developed to describe the electrification by impact of a sphere on a plane, and Fig. 2 shows the conceptual analogy between the electrification by the impact of the sphere and by the roller transfer process. The $(n\text{-}1)^{th}$, n^{th}, and $(n+1)^{th}$ rollers simultaneously contact the display panel and shift left with the frequency of v_{trans}/d, where d is the spacing between the shafts, and v_{tran} is the transfer velocity of the glass. The contact frequency of a specific location on the glass from the n^{th} to $(n+1)^{th}$ rollers is equal to v_{trans}/d.

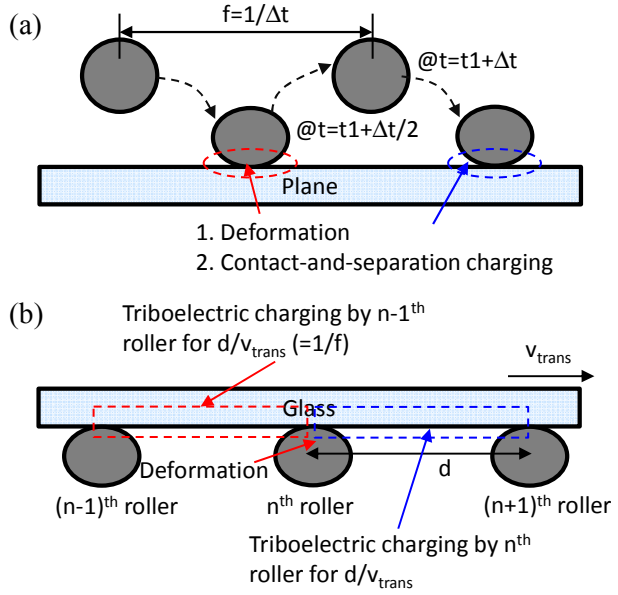

Figure 2: Conceptual Analogy between (a) Electrification by Impact of Sphere and (b) Electrification by Roller Transfer.

The E-field distribution on the display panel is calculated by numerically solving the 3D Poisson's equation with the boundary conditions of the charge distribution on the bottom of the display panel and the grounding conditions of the shafts. A commercially available 3D solver, CST EM Studio, was used in this work. It was assumed that the charges do not move on the surface via surface discharges.

2. Modeling of Mechanical Properties

The transmission of the glass on the roller transfer system is based on the rolling contact between the rollers and the glass. In the rolling contact, the contact area is divided into two domains: a sticking domain with the length of $2a'$ and a slipping/skidding domain with the length $(2a\text{-}2a')$. In the sticking domain, the relative velocity at the contact v_{tran}-$R\omega$ is zero, which means the pure rolling condition (static friction). In the slipping/skidding domain, the relative velocity is a nonzero value, which means the slipping condition (dynamic friction). In other words,

$$|\tau(x,t)| \begin{cases} < \mu p(x,t), \mathrm{x} \in \{\mathrm{stick}\} & (static\ frict.) \\ = \mu p(x,t), \mathrm{x} \in \{\mathrm{slip}\} & (dynamic\ frict.) \end{cases} \quad (5)$$

$$v_{trans} \begin{cases} = R\omega\ (pure\ rolling, static\ \ frict.) \\ > R\omega\ (skidding, dynamic\ frict.) \\ < R\omega\ (slipping, dynamic\ frict.) \end{cases} \quad (6)$$

where $2a$ is the contact length of two cylinders with parallel axes from the Hertzian equation, $\tau(x,t)$ is the tangential stress distribution, $p(x,t)$ is the Hertzian pressure distribution, μ is the friction coefficient according to the friction law of Coulomb, ω is the angular velocity, and R is the radius of the rollers [5, 6].

The ratio of each domain in the contact area depends on the relative velocity at the contact, and the areas of each domain are calculated using (7) and (8)

$$A_{sticking} = 2a' w_{roller} = 2\left(a - \frac{R}{\mu}\left|\frac{v_{trans} - \omega R}{v_{trans}}\right|\right) \cdot w_{roller} \quad (7)$$

$$A_{slipping\ /skidding} = A_{Hertzian} - A_{sticking} = \sqrt{\frac{16 F_n R'}{\pi E'} \cdot w_{roller}} - A_{sticking} \quad (8)$$

where F_n is the applied load, R' is the combined radius, E' is the combined elasticity modulus, and w_{roller} is the width of the rollers [5, 6]. The number of rollers beneath the glass is calculated every time, and then the force due to gravity is divided by the number of rollers to calculate F_n. Under pure rolling, i.e., the rolling without slipping condition (v_{tran}=$R\omega$), the area

of the sticking domain is equal to the Hertzian contact area, while the area of the slipping/skidding domain grows with increasing the relative velocity at the contact until it encompasses the entire contact area.

Because the skidding/slipping may stain the surface of the glass and cause display failures, the translational (transfer) and circumferential velocity should be under control in order to minimize the skidding/slipping during the display manufacturing process. However, the relative velocity at the contact inevitably increases/decreases during either acceleration ($v_{tran}<R\omega$) or deceleration ($v_{tran}>R\omega$) of the transfer velocity at both the beginning and the end of the roller transfer system, or during transfer velocity changes between two manufacturing units. Fig. 3 shows the conceptual diagram for the relative velocity at the contact and the corresponding contact areas of the sticking and the slipping/skidding domains during the roller transfer process of the display panels.

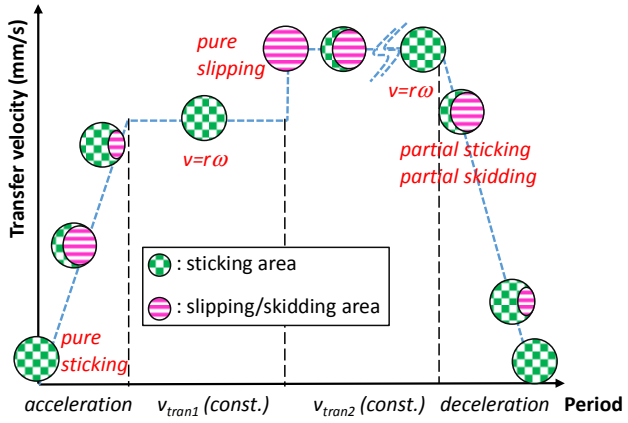

Figure 3: Conceptual Diagram for Relative Velocity at Contact and Contact Areas of Sticking and Slipping/Skidding Domains during Roller Transfer Process of Display Panel.

Triboelectric charges tend to increase as the acceleration/deceleration time of the transfer velocity decreases, or when there is a transfer velocity difference between manufacturing units as shown in Table 1 [2, 3]. There are still arguments on the physical causes of the increased charges, and potential reasons are increased contact area for charge transfer, localized frictional heating, material transfer, and so on [7–9]. In [9], the authors experimentally showed the effects of the contact area and the relative velocity at the contact on the triboelectric charges by changing the normal contact force and the rubbing velocity between two materials, respectively. In addition, the heat produced through friction is proportional to the contact area and the relative velocity at contact as shown in (9) [10]

$$Heat = \mu p A_{slipping\ /skidding}\ |v_{trans} - \omega R| \qquad (9)\ .$$

Based on the previously mentioned works, (2) is modified in order to consider the different triboelectric charging characteristics of the sticking and the slipping/skidding domains of the contact area as shown in (10)

$$q(n) = \qquad (10)$$

$$\begin{cases} q_{sticking}\ (n), & v_{trans} = \omega R \\ q_{slipping\ /skidding}\ (n), & \left|\dfrac{v_{trans} - \omega R}{v_{trans}}\right| = \dfrac{\mu a}{R} \\ A_{sticking} \cdot q_{sticking}\ (n) + A_{slipping\ /skidding} \cdot q_{slipping\ /skidding}\ (n), & 0 < \left|\dfrac{v_{trans} - \omega R}{v_{trans}}\right| < \dfrac{\mu a}{R} \end{cases}$$

where $q_{sticking}$ is the triboelectric charges between the glass and the rollers under the pure sticking condition, and $q_{slipping/skidding}$ is the triboelectric charges between the glass and the rollers under the pure slipping/skidding condition. Pure contact and separation electrification for the sticking domain, and pure frictional electrification for the slipping/skidding domain are assumed. The triboelectric charges for the partial sticking and partial slipping/skidding conditions are calculated by summing the multiplications of the triboelectric charges of the pure sticking and the pure slipping/skidding conditions by the areas of each domain, as shown in (10).

3. Modeling of Triboelectric Charging Characteristics Between Glass and Roller

In order to simulate triboelectric charging using (10), six constants n_0, q_0, and q_∞ values for the pure sticking and the pure slipping/skidding conditions should be experimentally determined by fitting with the measured triboelectric charges because they are functions of not only the known physical constants (such as the (effective) work functions, the contact capacitance, the effective contact area and frequency), but also the empirical fitting parameters (k_c, k_i, and k_l for the charging and the discharging efficiencies, humidity, surface roughness, manufacturing tolerance, and so on), as shown in (3)–(4).

An apparatus for determining the triboelectric charging between the glass and the rollers was developed in our research group. Material characterizations for the triboelectric simulations and correlation results between the measured and the simulated results are shown in section III. In this section, the triboelectric charging characteristics are fitted based on data in the published paper for insulating and dissipative materials [11].

Fig. 4 shows the modeled triboelectric charging characteristics between the glass and a single roller as the function of the number of the contacts for the purpose of simulation tool development. For the sample selected it was observed that the accumulated charges with the dissipative material were larger than those with the insulating material, and the charging time was also faster with the dissipative material [11]. The authors experimentally show that static dissipative surfaces can charge up insulating surfaces more efficiently than actual insulating surfaces in the case of friction between grounded static dissipative and insulating surfaces, and emphasize that triboelectric charging is highly related to the test arrangement and insulators must be evaluated case by case.

We analyzed the triboelectric charging behavior of the display panels during roller transfer processing by using the aforementioned electrical and mechanical models and the modeled triboelectric charging characteristics. In order to obtain the best possible prediction of the quantity of the triboelectric charges, fitting of the empirical parameters should be conducted with the same materials of the roller transfer system, which is discussed in section III in detail.

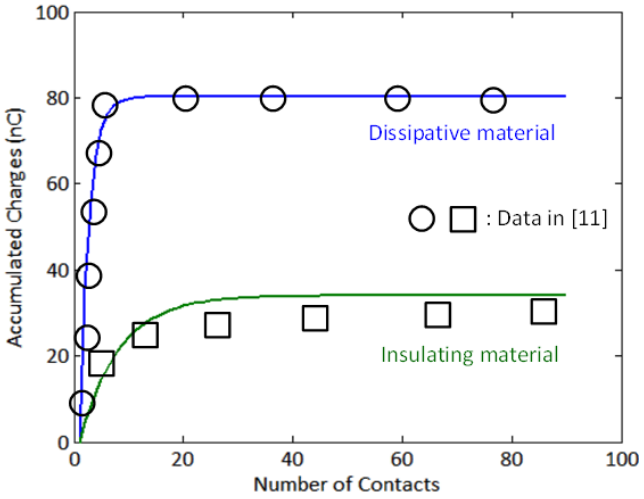

Figure 4: Modeled Triboelectric Charging Characteristics between Glass and Insulating/Dissipative Roller.

B. Simulated Triboelectric Charging of Display Panels

1. Charge Distribution Beneath Display Panel

Fig. 5 shows the schematic diagram of the roller transfer system of the display panels, where s_{shaft} and s_{roller} are the spacing between the shafts and the rollers, respectively, and $l_{display}$ and $w_{display}$ are the length and the width of the display panel, respectively. The values of w_{roller}, $l_{display}$, and $w_{display}$ are 10, 2200, and 1870, all in mm, respectively. Two different combinations for the values of d_{roller} and s_{shaft} are used; 60 and 150 (case 1), and 180 and 450 (case 2), all in mm, respectively. The transferred distance, $d_{transfer}$, is determined by the transfer velocity and the E-field calculation time.

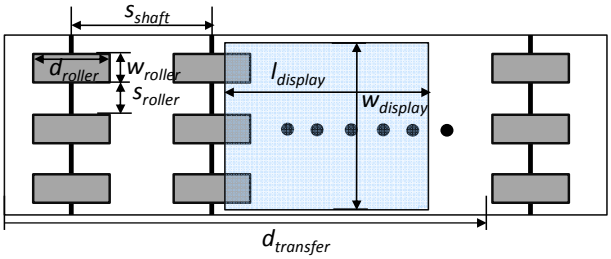

Figure 5: Schematic Diagram of Display Panel Conveyor.

Fig. 6 (a) shows the transient triboelectric charges on the bottom of the display panel at 5 and 15 sec with a 100 mm/sec transfer velocity, and rollers are assumed to be made of dissipative material. Fig. 6 (b) shows the transient triboelectric charges on the bottom of the display panel with the same condition, but now assuming insulating rollers. In both of cases, the diameter of the rollers and the spacing between the shafts is 60 mm and 150 mm, respectively. The maximum values of the triboelectric charge density with the dissipative and the insulating rollers at 15 sec are 10.5 nC/mm^2 and 3.8 nC/mm^2, respectively. The triboelectric charges with the dissipative rollers reach the saturation value of triboelectric charging faster than those with the insulating rollers.

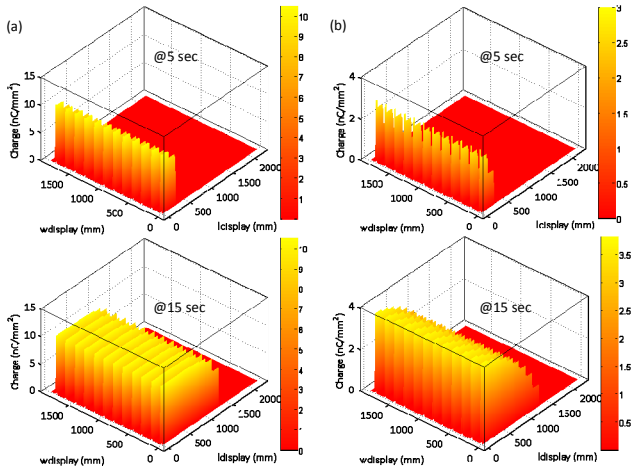

Figure 6: Transient Triboelectric Charge Distributions on the bottom of Display Panel at t=5 sec and t=15 sec with a 100 mm/sec transfer velocity (a) Rollers with Dissipative Material and (b) Rollers with Insulating Material.

2. E-field Distribution on Display Panel

Fig. 7 (a) and (b) show potential distributions on bare glass at 15 sec using a transfer velocity of 100 mm/sec. The insulating materials for the combination of case 1 and 2 are used. Three lines of rollers are considered.

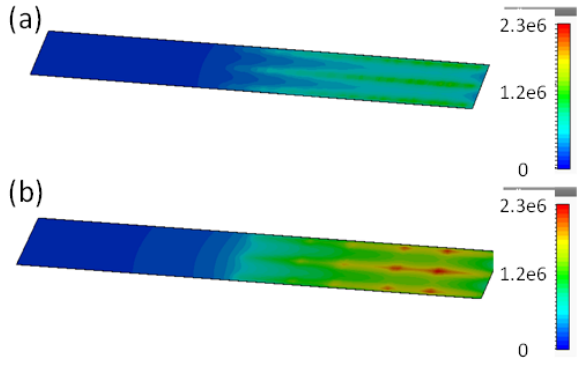

Figure 7: Potential Distribution at 15 sec (a) Case 1: d_{roller}=60 and s_{shaft}=150 mm and (b) Case 2: d_{roller}=180 and s_{shaft}=450 mm.

The peak potential of case 2 is 1.7 times higher than that of case 1 because the increased distance from the ground which is linearly proportional to the diameter of the rollers. Both of the cases are simulated under rolling condition without considering slipping.

III. Material Characterizations and Correlation between Measured and Simulated Results

A. Descriptions of Characterizations and Measurements Setup

Fig. 8 shows the fabricated apparatus for the characterizations of the roller and the glass materials and the measurements of the triboelectric charges of the roller transfer process, where the width and the transfer length of the apparatus are 61 cm and 188 cm, respectively. The stepper motors are used to control the rotational speed of the rollers and to control the height of the lift pins. The glass travels back and forth on the rollers by changing the rotational direction of the rollers, and the acceleration/deceleration time of the transfer velocity is also controllable. The lift pins are used to investigate the effect of the height of the glass from the ground on the electrostatic voltages on the glass and for charge creation during lift off from a metallic platform.

Several design parameters such as the diameter of the rollers, the spacing between the rollers, and the spacing between the shafts are mechanically adjustable. Insulating UHMW (ultra-high-molecular-weight) polyethylene was used to fabricate the rollers. Alkaline earth boro-aluminosilicate glasses are used for the characterizations of the materials and the measurements of the triboelectric charging.

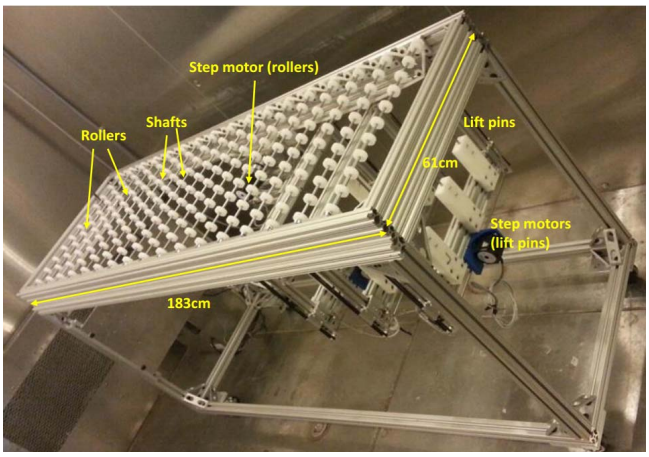

Figure 8: Fabricated Apparatus for Characterizations of Roller and Glass Materials and Measurements of Triboelectric Charging of Roller Transfer Process

The triboelectric charges were measured using a Faraday cup and the ES103 solid state electrometer from ESDEMC Technology LLC. The TREK model 347 electrostatic voltmeter was used to measure a voltage that leads to a field cancellation on the glass and the rollers [12]. In order to control the ambient humidity and temperature all of the characterizations and the measurements were conducted in the climate chamber with 30% humidity and 22°C ambient temperature [13]. In this work the 30% R.H. was selected, which is the lowest reliable level of humidity at 22°C which can be achieved in the climate chamber in summer months. Follow up experiments in the winter will allow lower humidity. The rollers and the glasses are cleaned using 91% isopropyl alcohol and preconditioned in the climate chamber for a minimum of twelve hours.

Firstly, the material characterizations were conducted by changing the number of the contacts, and based on the characterization results the required simulation parameters were extracted. As the next step, the multi-physics simulation of the triboelectric charging was conducted with different operating conditions and compared to measurements.

B. Characterization of Materials

In this work, the triboelectric charging characteristics under rolling without the slipping condition were studied. Because the triboelectric charges are dependent on the relative velocity at the contact and there are velocity changes due to the acceleration and the deceleration periods at both ends of the roller

transfer system, two-step measurements were conducted in order to extract the triboelectric charges of the sticking domain only. The proposed method can also be applied to the triboelectric charging characterizations for the rolling with slipping condition, which is a future work.

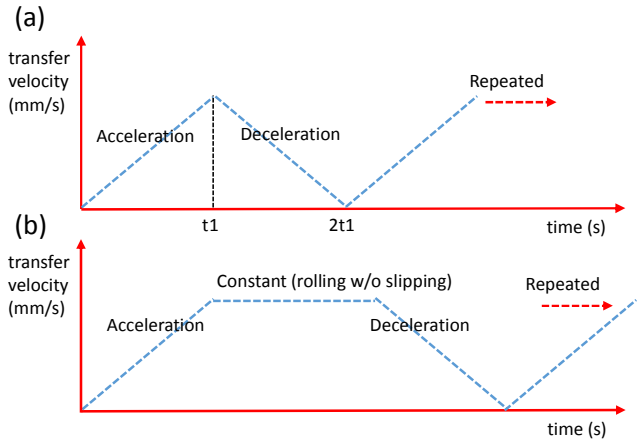

Figure 9: Transfer Velocity Conditions for Material Characterizations (a) with Acceleration and Deceleration Periods and (b) with Acceleration, Steady-state, and Deceleration Periods

First, the glass on the roller transfer system travelled back and forth with only the acceleration and the deceleration periods as shown in Fig. 9 (a), and the triboelectric charges on the glass were measured using the Faraday cup and the solid state electrometer. The triboelectric charges were measured again within the constant velocity period, as well as during the acceleration and the deceleration periods as shown in Fig. 9 (b). Using these two measured triboelectric charges, the triboelectric charges under the rolling without slipping condition were de-embedded.

Table 2: Driving Conditions of Roller Transfer System for Material Characterization

Driving condition		Parameter	Value
Transfer velocity	Acceleration (1 sec)	Rate (m/s^2)	1/10
		Displacement (m)	0.05
	Deceleration (1 sec)	Rate (m/s^2)	1/10
		Displacement (m)	0.05
	Steady-state (9 sec)	Velocity (m/s)	1/10
		Displacement (m)	0.9
Transfer distance	1 movement	FWD+RVS (m)	1.0+1.0
	Number of movements	(times)	30/60/90/……/ 420/450
	Number of contacts	(times)	600/1200/ 1800/……/ 8400/9000

The de-embedding was conducted by subtracting the triboelectric charges during the acceleration and deceleration periods from those having completed full periods. The driving conditions of the roller transfer system are summarized in Table 2.

Fig. 10 shows the measured triboelectric charge densities on the glass as the function of the number of contacts: the solid blue circles show the charge density with the driving conditions of the acceleration and the deceleration periods only, and the solid black triangles show the charge density with the driving conditions of the acceleration, the constant velocity, and the deceleration periods. The solid red squares show the de-embedded triboelectric charge density based only on the steady-state transfer velocity period. With less than 2400 number of contacts the measured triboelectric charges due to the acceleration and the deceleration periods are higher than those due to the steady-state transfer velocity period, however, the triboelectric charges due to the acceleration and the deceleration periods reached the saturated values of the triboelectric charging faster than the triboelectric charges due to the steady-state transfer velocity period.

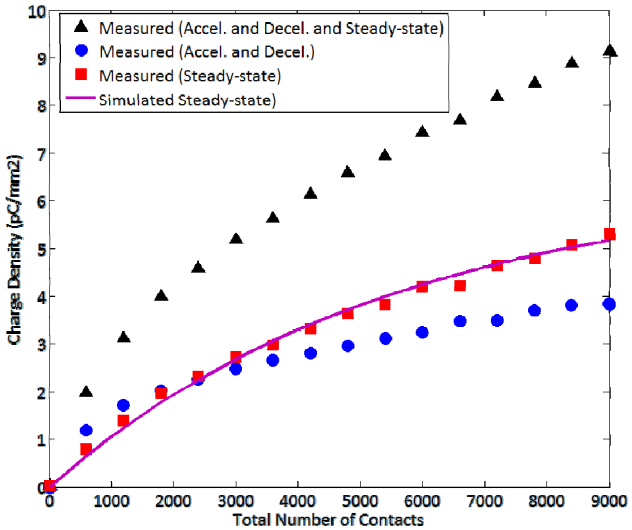

Figure 10: Measured (Solid Black Triangles, Solid Blue Circles, and Solid Red Squares) and Simulated (Purple Line) Triboelectric Charge Densities on Glass

The empirical parameters are extracted using the measured triboelectric charges. The purple line shows the simulated triboelectric charge density due to the steady-state transfer velocity period, and they show good agreements with the measured the triboelectric charge density due to the steady-state transfer velocity period.

C. Comparisons Between Measured and Simulated Results

Triboelectric charges due to the steady-state transfer velocity period were simulated with the extracted simulation parameters by changing the transferred distance. Fig. 11 shows the measured and the simulated total charges on the glass, where the solid red squares show the measured total charges and the purple line shows the simulated total charges, which show good agreement with the measured charges.

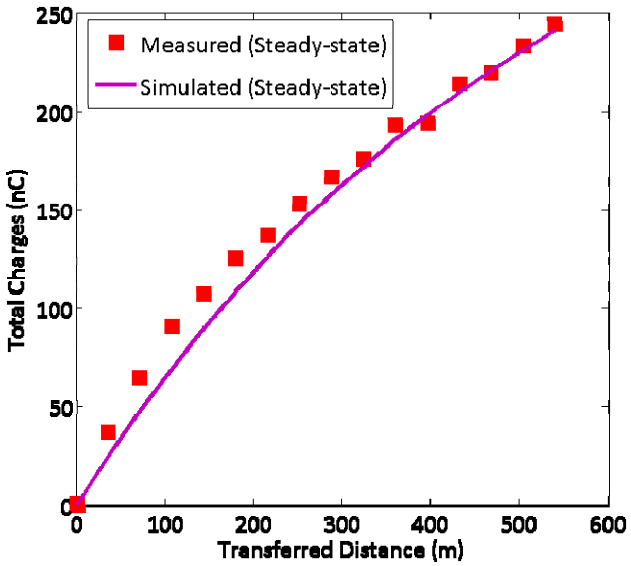

Figure 11: Measured (Solid Red Squares) and Simulated (Purple Line) Triboelectric Charges due to Steady-state transfer velocity period as Function of Transferred Distance

IV. Conclusions and Future Works

A simulation methodology for triboelectric charging of the roller transfer process is proposed. First, the methodology was verified based on previously published triboelectric characteristics of materials. The apparatus for the triboelectric charging characterizations of the glass and roller materials was developed, and material characterizations were conducted. Based on the material characterization results, the empirical parameters in the triboelectric charging equations were extracted and comparisons between the measured and the simulated triboelectric charges were conducted.

The developed simulation methodology is based on empirical equations. Systematic characterizations for triboelectric charging of glass on the roller transfer system using the developed apparatus would greatly helpful to optimize the empirical parameters extraction process and the equations themselves. In addition, the verification of the proposed triboelectric charging equations for the slipping/skidding domain is another future work.

Acknowledgements

The authors would like to acknowledge Samsung Display Co., Ltd., for supporting this project. The authors also would like to thank Jeffrey Birt for the design and fabrication of the roller transfer system and thank ESDEMC Technology LLC for providing the solid state electrometer.

References

[1] S. Matsusaka, *et al.*, "Triboelectric Charging of Powders: A review," Chemical Engineering Science 2010.

[2] D. –S. Kim, *et al.*, "Electrostatic Control and its Analysis of Roller Transferring Processes in FPD Manufacturing," EOS/ESD Symposium, 2013.

[3] J. Yoo, *et al.*, "Comparing Room Ionization Technologies in FPD Manufacturing," EOS/ESD Symposium 2012.

[4] W. D. Greason, "Triboelectrification of Wood with PTFE," Journal of Electrostatics 2013.

[5] J. B. Nielsen, *New Developments in the Theory of Wheel/Rail Contact Mechanics*, Technical University of Denmark 1998.

[6] V. L. Popov, "Rigorous Treatment of Contact Problems – Hertzian Contact," Contact Mechanics and Friction, Springer Berlin Heidelberg, 2010.

[7] P. M. Ireland, "The Role of Changing Contact in Sliding Triboelectrification," Journal of Physics D: Applied Physics 2008.

[8] W. R. Harper, *Contact and Frictional Electrification*, Oxford Press, 1967.

[9] L. Liu, *et al.*, "Frictional Electrification on Polymeric Flat Surfaces," Journal of Engineered Fibers and Fabrics 2013.

[10] L. M. Galantucci and L. Tricarico, "Thermo-mechanical Simulation of a Rolling Process with an FEM Approach," Journal of Material Processing Technology 1999.

[11] T. Viheriakoski, *et al.,* "Triboelectrification of Static Dissipative Materials," EOS/ESD Symposium 2012.

[12] http://www.trekinc.com/pdf/3002-field-voltmeter.pdf

[13] ESD ADV 11.2 – Triboelectric Charge Accumulation Testing, ESD Association 1995.